ALMA Memo #271

The Determination of Precipitable Water Vapour at Llano de Chajnantor from Observations of the 183 GHz Water Line

Guillermo Delgado[1,2]
Angel Otárola[1]
Victor Belitsky[2]
Denis Urbain[2]

[1]European Southern Observatory
[2]Onsala Space Observatory

THE DETERMINATION OF PRECIPITABLE WATER VAPOUR AT LLANO DE CHAJNANTOR FROM OBSERVATIONS OF THE 183 GHZ WATER LINE

Guillermo Delgado
Onsala Space Observatory / European Southern Observatory
Casilla 19001, Santiago 19, Chile
Email: gdelgado@eso.org

Angel Otárola,
European Southern Observatory
Casilla 19001, Santiago 19, Chile
Email: aotarola@eso.org

Victor Belitsky
Onsala Space Observatory
Radio and Space Science, S-41296 Göteborg, Sweden
Email: belitsky@ep.chalmers.se

Denis Urbain
Onsala Space Observatory
Radio and Space Science, S-41296 Göteborg, Sweden
Email: denis@ep.chalmers.se

Abstract - *At millimetre wave lengths the radio seeing is severely limited by the inhomogeneous distribution of water vapour. This is a fundamental limit to the resolution of terrestrial based millimetre wave interferometers. One way of overcoming this limitation is by using radiometric measurements of the brightness temperature of the sky to estimate the water vapour content of the atmosphere thus correcting the phase fluctuation in the observed wave front.*

Two radiometers to observe the 183 GHz water vapour line have been installed by the Onsala Space Observatory, Sweden, at Llano de Chajnantor, northern Chile. This as part of the site testing work carried out by the European Southern Observatory in collaboration with the National Radio Astronomy Observatory (NRAO) and other European organisations in the frame of the Atacama Large Millimeter Array project (ALMA).

Here we present a description of the radiometers and their stability. Also we show a method to estimate the amount of precipitable water vapour (PWV) from antenna brightness temperature measurements at three frequencies close to the water line transition at 183.31 GHz. The data is fitted to a simple atmospheric water line emission model, starting from ground-level weather information. Data has been collected and analysed continuously, starting September 1998 at Llano de Chajnantor.

The value of PWV obtained with the 183 GHz radiometer was correlated with radiosonde measurements and atmospheric opacity measured at 225 GHz.

The correlation with opacity measurements at 225 GHz is very good, giving confidence in the estimated value of PWV. In the case of radiosonde measurements, a systematic error in the determination of relative humidity (RH) by the radiosonde detectors was observed. More data is expected from the radiosonde manufacturer to further proceed with the analysis.

1. Introduction

The transparency of the atmosphere at millimetre wavelengths is severely affected by absorption due to its molecular constituent. In particular the water vapour content is a fundamental limitation, not only because it attenuates the incoming signal, but also because water vapour produces fast changes in the diffraction index of the air, changing the electrical path length and thus affecting the phase of the incoming wave front.

To a first order approximation water vapour is distributed exponentially with a scale height of 1 to 2 km [1], but, due to imperfect mixing, water vapour is not distributed evenly and moves in layers ("bubbles" or "pockets"), thus creating the equivalent to turbulence in optical astronomy. This is particularly relevant in interferometry where an image must be reconstituted from the signal coming from several telescopes separated by a physical distance.

Since the path length variations are, to a first order, proportional to the amount of precipitable water vapour (*PWV*), one way of overcoming this problem is to measure the variation of the content of *PWV* to infer the path length variations and correct the incoming phase accordingly.

By using a multichannel radiometer to measure the sky brightness at three frequency bands, close to the water line at 183 GHz, information on the line shape and intensity can be retrieved. The amount of *PWV* can be obtained though fitting of an atmospheric water line emission model to this line shape.

The *Onsala Space Observatory*, representing Sweden in a consortium of European countries interested in the development of a sub-millimetre array in the Southern Hemisphere, has designed and built through the *Advanced Receiver Group* at *Chalmers University of Technology*, in collaboration with the *Mullard Radio Astronomy Observatory* (MRAO), Cavendish Laboratory, two radiometers for the water vapour line at 183.31 GHz. The radiometers are similar to the ones described by Wiedner [2]. The two radiometers have been installed at Llano de Chajnantor in Northern Chile at an altitude of 5,000 m; they are situated at the ends of a 300-m baseline of a 12 GHz interferometer. The idea is to correlate the atmospheric phase fluctuations as determined from both systems.

The instruments are flexible enough to allow, under computer control, a complete movement of the beam across the sky. They run autonomously and are controlled by a host PC. An additional remote PC running a LabView program, under Windows OS, retrieves and stores the data. From these data, recovered on a monthly basis during regular visits to the site, it is possible to infer the water vapour content and opacity.

This report concentrates in the results of the first installed radiometer at Chajnantor. This is the one located at the West side of the interferometer baseline.

2. The 183 GHz radiometer

The 183 GHz radiometer is a double sideband heterodyne receiver. The detection bands are spaced 1.2, 4.1, and 7.6 GHz away from the line centre, with bandwidths 0.4, 1.1, and 1 GHz respectively. The mixer is a room temperature Schottky type and the local oscillator (LO) is a free running, 91.7 GHz Gunn oscillator. The position of the intermediate frequency (IF) channels is overlaid on a typical water line shape in Figure 1. During the first six months of operation the centre IF channel did not have a filter thus having a bandwidth of nearly 3 GHz without a well defined channel centre, this was changed in March 1999 with the addition of a filter defining the actual parameters.

The mixers, developed at the *Rutherford and Appleton Laboratories,* are sub-harmonically pumped. The use of this type of mixers has two main advantages: there is no need for an external bias voltage and there is also no need to double the Gunn oscillator frequency to pump the mixer. The resulting radio frequency (RF) circuit is simpler and more reliable. The receiver noise temperature is measured to be about 1,500 K in each

channel.

The IF and RF electronics, including the Gunn oscillator and mixer are mounted in a temperature stabilised aluminium plate.

The radiometer is continuously calibrated by switching the beam between the sky and two reference black bodies at temperatures of about 40 and 90 ºC.

The output from the broadband mixer is split into the three IF bands and, after additional filtering, they are detected in diode total power detectors. These signals are voltage to frequency (V/F) converted to be further processed digitally. A more detailed description of the radiometers can be found in [3].

2.1. Calibration loads stability

The radiometer is calibrated using two loads, a warm load at about 40 ºC (314 K) and a hot load at about 90 ºC (365 K). The temperature control is an on-off feedback loop that works by heating the loads to their reference temperature. The design is the same one described for the MRAO radiometers in [2].

The loads are temperature stable to within ±0.02 K in a period of 9 hours. During a 24-hour period the temperature variations reach 0.1 K for the hot load and 0.2 K for the warm load. With these values, the load difference is stable to 51.50±0.02 K during 9 hours, as shown in Figure 2. During a 24 hour period the difference is stable to within 0.1 K.

A "snapshot" of 10 minutes shows that the temperature difference presents a ripple of 2.5 mK amplitude a period of 0.16 Hz (Figure 3). This can be traced to a ripple of about 1 mK in the hot load and 1.5 mK in the warm load. The ripple in the two loads is 180º out of phase and thus sums up during the waveform subtraction.

It remains to be determined if this noise is due to a temperature associated oscillation (due to the feedback), or due to beating of two closely adjacent frequencies, thus pointing to crosstalk in the V/F converters. In any case, the amplitude of this ripple does not affect the calibration.

2.2. Gunn diode stability

The free running Gunn diode local oscillator is not phase locked because of the broadness of the water line and because the line is symmetric. Hence, any instability is compensated by the DSB detection. In addition, the frequency stability of the oscillator is better than 4 MHz/ºC, so by regulating the LO temperature to within 1 ºC, we obtain a negligible 0.004% frequency drift.

The Gunn diode bias voltage is stable to 9.204±0.001 volts during a 9 hour period. In a 24 hour period the voltage drifts 0.06 volts from the nominal bias voltage. In a Gunn rated at 300 MHz/volt this translates to a frequency drift of 17 MHz from the nominal frequency that, at 183 GHz, is equivalent to a 0.02% frequency drift.

2.3. Total power output stability

To check the stability of the 183 GHz radiometer a measurement was done with a piece of microwave absorbing material (Eccosorb) filling the input beam of the radiometer. This material acts as a blackbody emitting at a temperature equivalent to the ambient temperature, since the Eccosorb is in thermal equilibrium with the surroundings.

The test was done recording data for more than an hour. The ambient temperature was simultaneously registered using the Davis weather station with a time resolution of 1 second.

The antenna brightness temperature on the three channels of the radiometer is similar, with the average ratio between pairs of channels of 1.0002±0.0009 during the total test time. This is to be expected in a well-calibrated system, since we assume the Eccosorb to have a flat radiation spectrum over the observed fre-

quency range (183.31±7.6 GHz).

The measured brightness temperature can also be correlated with the ambient temperature. The ratio between measured ambient temperature and the calibrated brightness temperature measured at the Eccosorb is 1.02±0.01

The data was analysed using the Allan variance method, and the result is shown in Figure 4. It can be seen that the radiometer is white-noise dominated up to approximately 200 seconds, while the random-walk noise starts to dominate this radiometer at a time of about 1000 seconds (16 minutes). The actual integration time is less than 400 ms at each cycle phase (loads and sky), so we are certain to be operating at the white noise dominated regime.

3. Determination of the sky brightness temperature from the radiometer data

At millimetre wavelengths we have that for most temperatures $h\nu << kT$, also known as the Raleigh-Jeans regime, and the brightness temperature is proportional to the blackbody emission temperature. This is valid for most temperatures encountered here, except the background emission that can not be represented by the Raleigh-Jeans approximation. Under these conditions, assuming that we are observing a sector of the sky free from emissions other that the background radiation, the brightness temperature of the atmosphere, at a frequency ν, is given by:

$$T_b(\tau_\nu) = T_{atm}\left(1 - e^{-\tau_\nu}\right) + \frac{h\nu}{k}\frac{1}{e^{h\nu/kT_b} - 1}e^{-\tau_\nu} \qquad (1)$$

where:

- h: Planck's constant, $6.626076 \cdot 10^{-34}$ [Js]
- k: Boltzmann's constant, $1.38066 \cdot 10^{-23}$ [J/K]
- T_B: Cosmic background temperature, 2.7 [K]
- τ_ν: Opacity or optical depth at frequency ν.
- T_{atm}: Effective temperature of the atmosphere [K]

The opacity τ_ν is a dimensionless function of the frequency ν, defined as the integral of the unit volume absorption coefficient k_ν along the total path s through the atmosphere.

$$\tau_\nu = \int_0^s k_\nu \, ds \qquad (2)$$

The coefficient k_ν is equal to the sum of the unit volume absorption coefficients, at frequency ν, corresponding to each of the gases constituting the atmosphere along the line of sight. These coefficients describe the interaction between the electromagnetic radiation and these molecular components and they will be functions of the density of these constituents as well as of the pressure and temperature of the media.

If a zenith optical depth is defined, then the opacity at an elevation angle α can be approximated by:

$$\tau_\nu = \frac{\tau_0}{\sin\alpha} \qquad (3)$$

where τ_0 is the zenith optical depth and we have dropped the frequency dependence, assuming that we remember this.

Equation (1) can the be written as function of the elevation angle as:

$$T_b(\alpha) = T_{atm}\left(1 - e^{-\tau_0/\sin\alpha}\right) + \frac{h\nu}{k}\frac{1}{e^{h\nu/kT_b} - 1}e^{-\tau_0/\sin\alpha} \qquad (4)$$

Even with the best optics, we can not guarantee that the radiometer will couple with 100% efficiency to the sky and that no spillover radiation will be detected by the radiometer. In general, the response of a radiometer, the so-called antenna temperature, is given by

$$T_A(\alpha) = \eta T_b(\alpha) + T_{amb}(1 - \eta) \qquad (5)$$

where η is the coupling efficiency to the sky.

The first term of (5) represents the atmosphere brightness temperature, reduced by the coupling efficiency of the radiometer to the radiation coming from the sky, this term is detected through the main beam of the antenna. The second term represents detected power through sidelobes and scattering from the ground, optics and surrounding structures at ambient temperature.

A coupling efficiency of $\eta = 97\%$ was found for the first working radiometer by performing measurements of antenna temperature at different elevation angles α, and fitting least squares to the antenna temperature as function of elevation.

4. Atmospheric water line model fitting

In equation (4), the term

$$T_{brightness} = T_{atm}\left(1 - e^{-\tau_0/\sin\alpha}\right) \qquad (6)$$

represents the total effective brightness temperature of the atmosphere that, at 183 GHz, is due mainly to the thermal emission of the water vapour line. The strength and shape of the water vapour line depends not only on the amount of water vapour, but also on the distribution of temperature, pressure, and water vapour density through the atmosphere. To calculate the atmospheric emission due to the water vapour, we use the radiative transfer model with the atmosphere divided in several layers and the radiation travelling from the higher layers down.

The atmosphere is divided in layers of 200 m each; integrating to a maximum altitude of 8,000 m. At each layer, the brightness temperature of the atmosphere is calculated as the sum of two terms: the radiation entering that layer from the layers above (not counting the background radiation) and the blackbody emission of that layer. Each layer is assumed to be of uniform density and at thermal equilibrium, with these conditions changing between layers.

At each layer the brightness temperature is given by:

$$T_{brightness}(j) = T_{brightness}(j-1)e^{-k_\nu \Delta s} + T_j\left(1 - e^{-k_\nu \Delta s}\right) \qquad (7)$$

Where:

- $T_{brightness}(j)$: Brightness temperature of the radiation entering the j-layer from layers above
- k_ν: Absorption coefficient at the j-layer
- Δs: Distance travelled inside the j-layer
- T_j: Blackbody temperature of the j-layer

To calculate the brightness temperature at each layer, we follow the procedure outlined by Waters [4]. The layer absorption coefficient k_ν is calculated as the sum of two components: one due to the water line emission and the other is an empirical correction term. The line shape utilised is the Ben-Reuven kinetic line shape.

The total opacity is calculated as the integral of the absorption coefficients and approximated by the sum:

$$\tau_\nu = \int_0^s k_\nu \, ds \approx \sum_{all\ layers} k_\nu \, \Delta s \qquad (8)$$

Ground based meteorological data (atmospheric pressure, temperature, and relative humidity (RH)) serves as input to the model. The pressure and temperature are assumed to vary with height according to the expressions given in section 6. The water vapour density is calculated, as function of height, starting from the value of RH at ground level. The model is run an a line strength is calculated, this value is compared with the actual measured antenna temperature, using equation (4), and iteration over the water vapour density is done until a successful fitting is achieved. Once a water vapour density value is determined, the amount of *PWV* contained in the atmospheric column observed by the radiometer beam is estimated by using:

$$PWV = \int_0^s \rho_0 \, e^{-s/h} \, ds \qquad (9)$$

where:

- ρ_0: Water vapour density at ground level [gr/m^3]
- h: Scale height of the water vapour distribution [km]

The *PWV* estimation is very sensitive to the scale height used for the water vapour distribution. This parameter should be determined for Chajnantor before an accurate *PWV* value can be estimated.

A typical fitting can be seen in Figure 5, where the filled dots indicate the channel position and its measured value, whereas the solid line correspond to the best fitting using available ground meteorological data.

Figure 6 is the plot of the antenna temperature output, for each channel, as function of the estimated amount of *PWV*. The 1.2 GHz IF channel saturates for values of *PWV* greater than 1.5 mm, while the 7.6 GHz IF channel remains closer to a linear function of the amount of *PWV*.

The data in Figure 6 was accumulated over the month of October 1998, using a scale height for the water vapour distribution of 1.5 km and a wide a range of meteorological variables:

- Ambient temperature: -14/+6 [ºC]
- Pressure: 553/563 [mbar]
- Relative humidity: 3/90 [%]
- *PWV*: 0.25 to 6.3 mm

Under these conditions, the antenna temperature of the 7.6 GHz IF channel can be fitted accurately with a second order polynomial (Figure 7) giving an estimation for the amount of *PWV* in millimetres as function of the antenna temperature of this channel:

$$PWV = -0.29275 + 3.5848 \cdot 10^{-2} \, T_A + 1.0646 \cdot 10^{-4} \, T_A^2 \qquad (10)$$

The use of the antenna temperature value of the 7.6 GHz IF channel to obtain an initial seed for the amount of *PWV*, instead of estimating it through iterations starting from RH humidity measurements at ground level, increases the speed of calculation. A value of *PWV* can be obtained in less than a second of calculation in a PC compatible, this enables on-line phase corrections if needed.

5. Weather parameters

Two weather stations are working at Chajnantor. They measure: air temperature, solar radiation, atmospheric pressure, RH, and wind speed and direction. Their main characteristics are detailed in Table 1.

The weather stations include a data logger that, with the actual sampling rate of one reading every hour, can store 42 days of data. The wind sensors are atop a 4-m mast and the other instruments are installed in a ventilated shelter to protect them from direct solar radiation. Temperature, atmospheric pressure, and relative humidity data provides the basic input for the analysis of the data obtained with the 183 GHz radiometer.

By placing the two weather stations close to each other and comparing their outputs for a extended period we obtain a relative difference between them of 0.5% in RH, 0.15 ºC in temperature, and 3.5 mbar in atmospheric pressure.

The difference in RH and temperature does not affect the outcome of the water line atmospheric model. In the case of pressure changes, we have that at higher ground pressures the water line becomes broader and less intense for the same amount of *PWV* [2]. However, simulations show that a difference of ±5 mbar produces no difference in the shape of the line with all other parameters remaining constant.

6. Radiosonde correlation

Starting in October 1998 radiosondes have been launch from Chajnantor in a collaborative effort between NRAO, Cornell University, Center for Astrophysics at the Smithsonian Astrophysical Observatory and ESO. The radiosondes used are type Intellisonde model IS-5A-1680 from A.I.R. Inc. [5]. We compared the amount of *PWV* derived from 16 radiosonde launches during the second half of 1998 from Llano de Chajnantor with the amount of *PWV* derived from radiometer measurements taken at the same time

To obtain the amount of *PWV* from radiosonde measurements we integrated the water vapour column over a height of 8 km above ground. The only parameters needed are RH and temperature, obtained at about every 5 m at normal balloon ascension rates [6].

In the atmospheric water line model used to calculate the amount of *PWV* from the radiometer data, the ground meteorological data is used to infer the distribution of meteorological parameters as function of height. The radiosonde profiles are a very good opportunity to validate the meteorological parameter distribution models.

The pressure model used in the atmospheric model calculations assumes an exponential decay with a scale height *H* according to Houghton [7], given by:

$$P(h) = P_0 \, e^{-\int_0^h \frac{1}{H(h)} dh} \qquad (11)$$

$$H(h) = \frac{R T(h)}{M_d \, g} \qquad (12)$$

where

- P_0: Pressure at ground level [mbar]
- R: Molar gas constant, 8.31451 [J mole^{-1} K^{-1}]
- M_d: Molecular weight of “dry” air, 0.02896 [kg mole^{-1}]
- g: Gravitational constant, 9.8 [m s^{-2}]

This model compared with radiosonde measurements gives an agreement better than 0.5% at 8,000 m, limit of the integration for *PWV* determination.

For the temperature, the radiosonde sensors have an accuracy of 0.3 °C, with a resolution of 0.1 °C, according to the manufacturer. The atmospheric temperature distribution model, used in the radiometer data reduction, is the one by Thompson *et al*. [8]. Since this model predicts a different temperature distribution to the one given by the standard atmosphere [9], we compared both methods. No significant difference for the

amount of *PWV* as determined using both temperature profiles could be seen, so we keep the Thompson *et al*. Model given by,

$$T(h) = T_0 \left(0.98\right)^{h[\mathrm{km}]} \qquad (13)$$

Where the temperature drops by 2% from a temperature T_0 at ground level, with a scale height of 1 km.

The difference between actual temperature data, taken by the radiosonde, and the one predicted is about 2%, in the worst case at 8,000 m the integration limit.

The correlation is good between the PWV as determined by radiometric measurements and radiosonde measurements, but presents a non-unity slope and an offset because of systematically lower values of *PWV* determined with the radiosonde method as shown in Figure 8.

The radiosonde humidity sensors have an accuracy of 2% according to the manufacturer [5]; nevertheless, analysis of the data indicated that the radiosonde humidity sensors were underestimating the real RH value. This effect was latter confirmed by A.I.R. Inc., the manufacturer of the sensors, and attributed to solar radiation on the RH sensor [10]. The slope might be explained by the effect of day-time launches combined with uncorrected day-time launches. No more analysis will be done until better data is available from the manufacturer.

7. 225 GHz opacity correlation

A 225 GHz tipping radiometer was installed in 1995 at Llano de Chajnantor by NRAO. The atmospheric transparency is determined by measuring the sky brightness at different elevation angles [11]

To correlate the 225 GHz opacity measurements we took the raw data for the month of October 1998 (available at [12]) and discarded the bad data, usually overflow (-999) or values of opacity greater than unity. During this time the radiometer was pointed to zenith.

The 183 GHz measurements are taken one every 2 seconds but the data reduction program, that calculates the *PWV*, reduces the sampling to one *PWV* value every ten minutes. The 225 GHz tipping radiometer takes one opacity reading every 10 minutes [13]. These two data bases do not agree in the time stamp.

To relate the two data sets, we define the time stamp of the opacity measurements as the reference and extrapolated a *PWV* value from the two nearest *PWV* values, adjacent to the time of the opacity measurement.

The final data set compromised over 2,600 data points covering about 26 days of October, 1998. There is some downtime in the 225 GHz tipping radiometer, but the coverage is uniform within the month.

Figure 9 shows the correlation between the atmospheric opacity at 225 GHz and the amount of *PWV* estimated from 183 GHz radiometric measurements. The plot also shows the correlation between the two quantities as estimated from the Liebe '93 model for a site at 5,000 m [14], with an ambient temperature of 0 °C, an atmospheric pressure of 553 mbar, and assuming a scale height factor of 2.0 km for the water vapour distribution. This result depends on the atmospheric transparency model used and should be refined.

A second order polynomial fit to the experimental data gives a relation between opacity at 225 GHz and *PWV*:

$$\tau_{225\,GHz} = 6.7787 \cdot 10^{-3} + 4.0757 \cdot 10^{-2}\, PWV + 9.59 \cdot 10^{-4}\, PWV^2 \qquad (14)$$

In comparison Liebe's model predicts, for a scale height of 2.0 km:

$$\tau_{225\,GHz} = 5.449 \cdot 10^{-3} + 4.161 \cdot 10^{-2}\, PWV + 8.981 \cdot 10^{-4}\, PWV^2 \qquad (15)$$

8. *PWV* variations at Chajnantor

A simple method to estimate the amount of *PWV* has been developed. The method is fast and its consistency has been checked by correlating the result against independent estimations of *PWV*.

Data has been collected and analysed in Llano de Chajnantor, starting in September 1998. The time distribution of *PWV* shows clearly the diurnal cycle, as can be seen in Figure 10. In addition, the quartiles for this period are shown in the same figure.

Reduced *PWV* data for Chajnantor is available at [15].

9. Future work

The scale height for the water vapour density distribution needs to be determined for the site of Chajnantor in order to have an accurate value for the estimation of *PWV*. The exponential dependence of *PWV* on the value of scale height introduces big variations on the estimated value of *PWV* with all other conditions unchanged.

The correlation between the amount of *PWV* determined from radiosonde measurements and from 183 GHz radiometric measurements needs to be determined again. This time, night-time measurements should be done to confirm the effect of solar radiation affecting the accuracy of the RH sensors. Also we received from A.I.R. Inc., the radiosonde manufacturer, specially made radiation shields to be installed over the RH sensors during day-time launches.

More data should be correlated with the 225 GHz tipping radiometer, especially to improve the statistics for higher values of *PWV*. Data should be analysed separately for day time and night time observations to check for the claimed variability of the scale height for the *PWV* distribution [13].

Zammit and Ade have found that the excess zenith sky attenuation is better fitted using an empirical correction term given by Rice and Ade [16], instead of the one given by Gaut and Reinfenstein [4] that we are using. This should be revised for its possible influence.

More work needs to be done to characterise the instrumental noise of the radiometers, in order to isolate the atmospheric noise, and thus get a better idea of the “seeing” over Chajnantor.

Acknowledgements

Professor Roy Booth from *Onsala Space Observatory* has been instrumental in the successful installation of these radiometers. Martina Weidner formerly at MRAO, now at the Harvard-Smithsonian Center for Astrophysics, kindly provided the basic software for the atmospheric model, Professor Richard Hills from MRAO is acknowledged for always been ready to answer any question.

Lars-Åke Nyman, from SEST. is acknowledged for a careful reading of the manuscript and his many useful comments that have improved the readability of this work.

Bryan Buttler from NRAO is acknowledged for his help calculating the 225 GHz opacity as function of *PWV*.

Funding for the project came out of the budget of Onsala Space Observatory, provided by the Swedish Natural Science Council (NFR).

References

[1] S. Radford y M. Holdaway, "*Atmospheric Conditions at a Site for Submillimeter Wavelength Astronomy*", in *Advanced Technology MMW, Radio, and Terahertz Telescopes*, T. Phillips ed., SPIE 3357, pp. 486-494, 1998.

[2] M. Wiedner, PhD thesis, 1998.

[3] http://gard.rss.chalmers.se/sitetest/index.htm

[4] J. Waters, "Absorption and emission by atmospheric gases," in *Methods of Experimental Physics*, M. Janssen (Ed.), Vol. 12B, pp. 142-176, 1976.

[5] Intellisonde model IS-5A-1680, http://www.airmfg.com/RT.htm.

[6] A. Otárola and G. Delgado, "Correlation between *PWV* estimated from 183 GHz radiometric and radiosonde measurements," in preparation.

[7] J. T. Houghton, *The Physics of Atmospheres*, Cambridge University Press, 1986.

[8] A. Thompson, J. Moran, and G. Swenson, *Interferometry and Systhesis in Radio Astronomy*, Krieger Publishing Company, 1994.

[9] J. Iribarne and W. Godson, *Atmospheric Thermodynamics*, D. Reidel Publishing Co., 1973.

[10] R. Shelhorn (rons@airmfg.com), A.I.R. Inc., private communication.

[11] M. McKinnon, "Measurement of Atmospheric Opacity due to Water Vapor at 225 GHz," MMA Memo # 40, 1987.

[12] http://www.tuc.nrao.edu/mma/sites/Chajnantor/.

[13] M. Holdaway, M. Ishiguro, S. Foster, R. Kawabe, K. Kohno, F. Owen, S. Radford, and M. Saito, "Comparison of Río Frío and Chajnantor Site Testing Data," MMA Memo # 152, 1996.

[14] H. Liebe, AGARD 52nd Meeting, Palma de Mallorca, Spain, 1993.

[15] http://puppis.ls.eso.org/lsa/htmls/rx183.html.

[16] C. Zammit and P. Ade, "Zenith atmospheric attenuation measurements at millimetre and submillimetre wavelengths", Nature, Vol. No. 293, pp. 550-552, 1981.

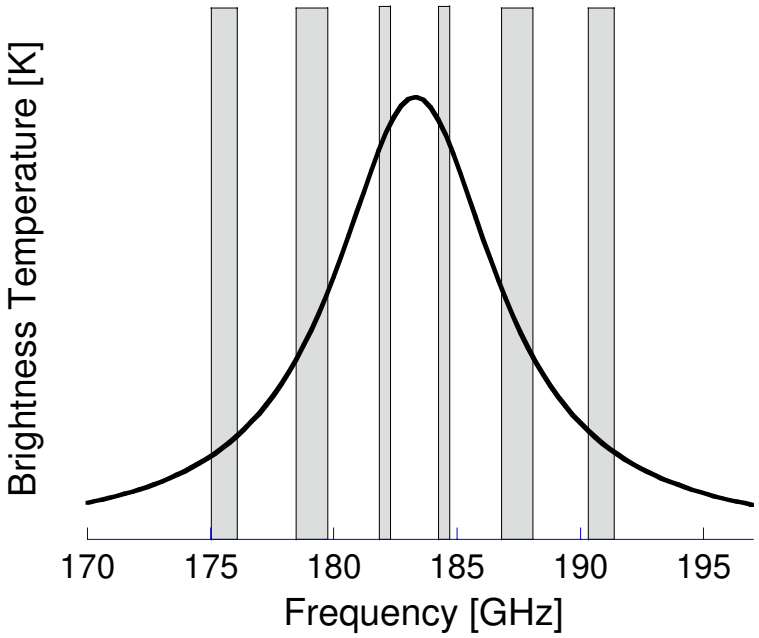

Fig. 1 Measured channels and their bandwidths over a simulated water vapour line.

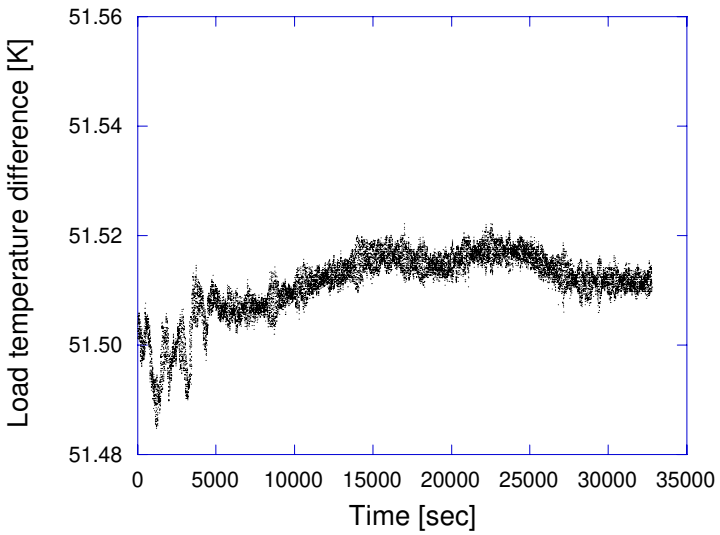

Fig. 2 Loads temperature difference in a 9 hour period

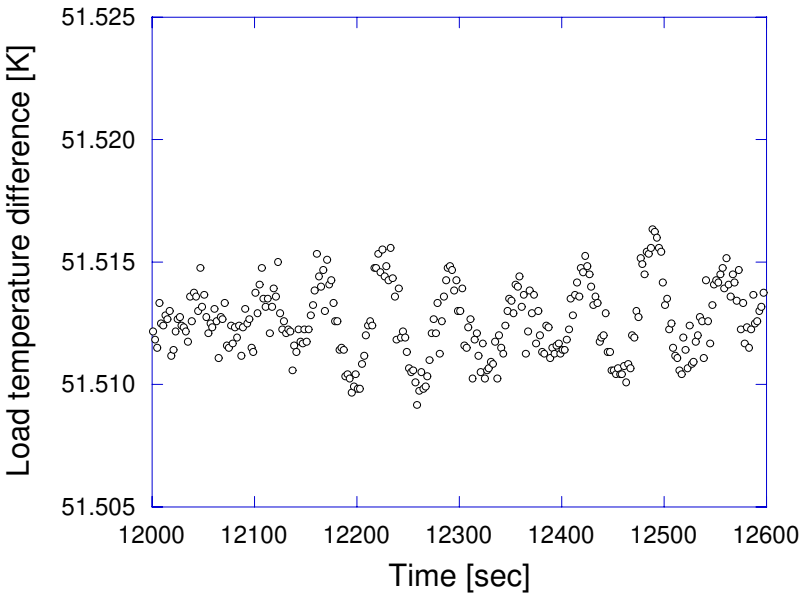

Fig. 3 Loads temperature difference in a 10 minutes period.

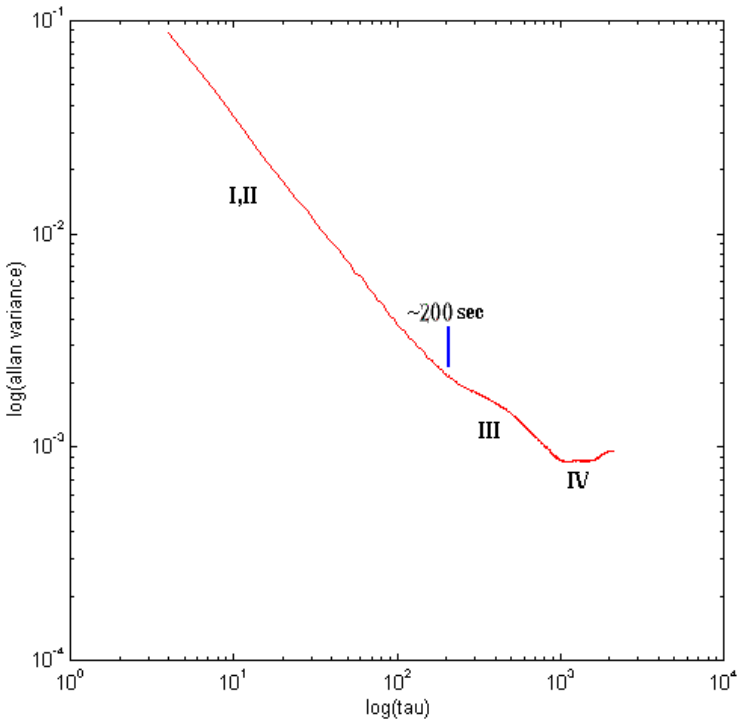

Fig. 4 Allan variance for the brightness temperature of the 183 GHz radiometer measuring an Eccosorb at ambient temperature.

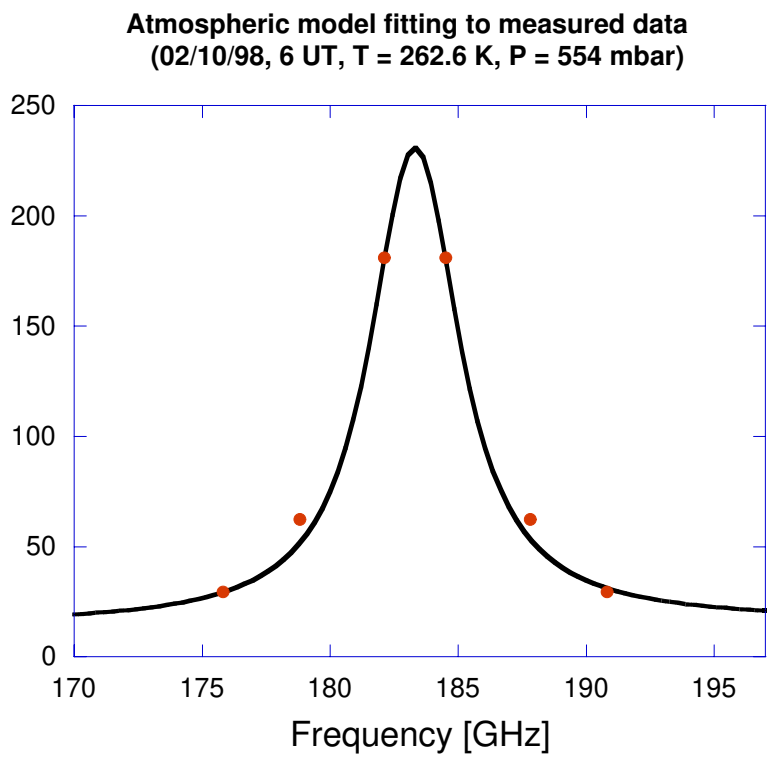

Fig.5 Fitting of the atmospheric water line model prediction to the measured antenna brightness temperature.

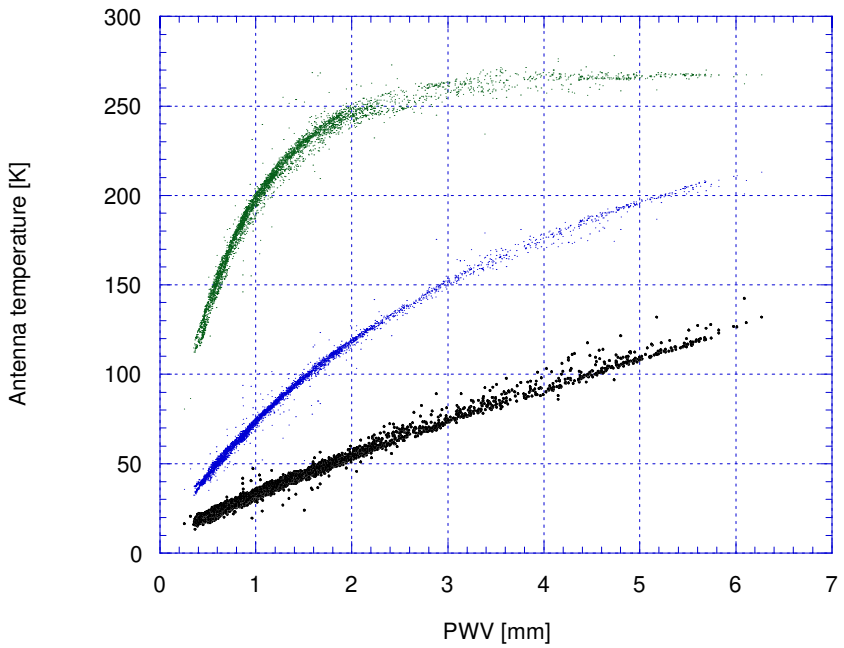

Fig.6 Antenna temperature for each of the three IF channels, the upper curve is the 1.2 GHz IF channel, the centre curve is the 4.1 GHz IF channel, the lower curve is the 7.6 GHz IF channel.

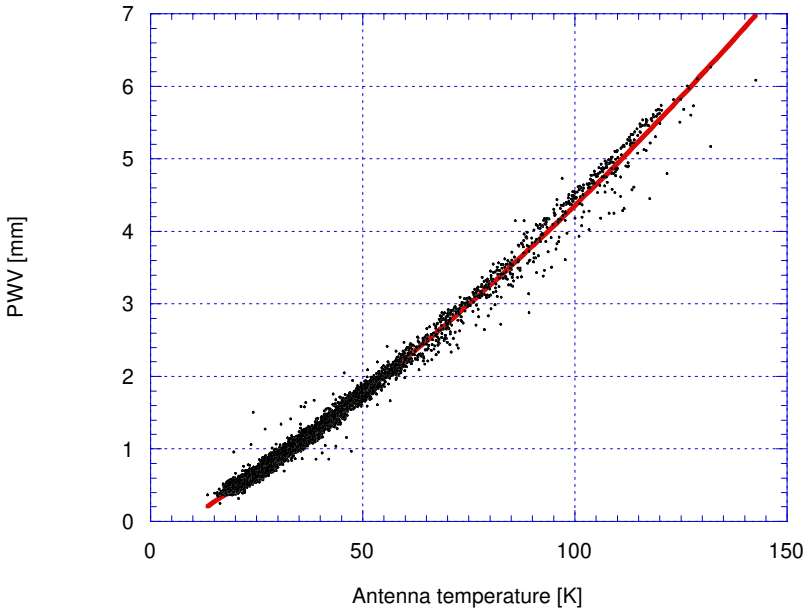

Fig. 7 Amount of *PWV* [mm] as function of antenna temperature of the 7.6 GHz IF channel with the fitted second order polynomial.

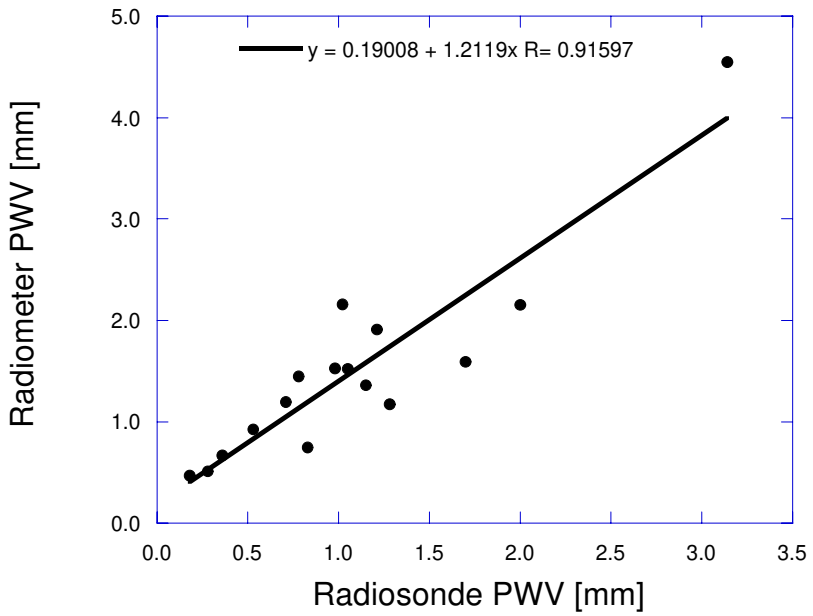

Fig.8 Correlation between the amount of *PWV* derived from radiosonde vertical profiles and radiometer determined *PWV*

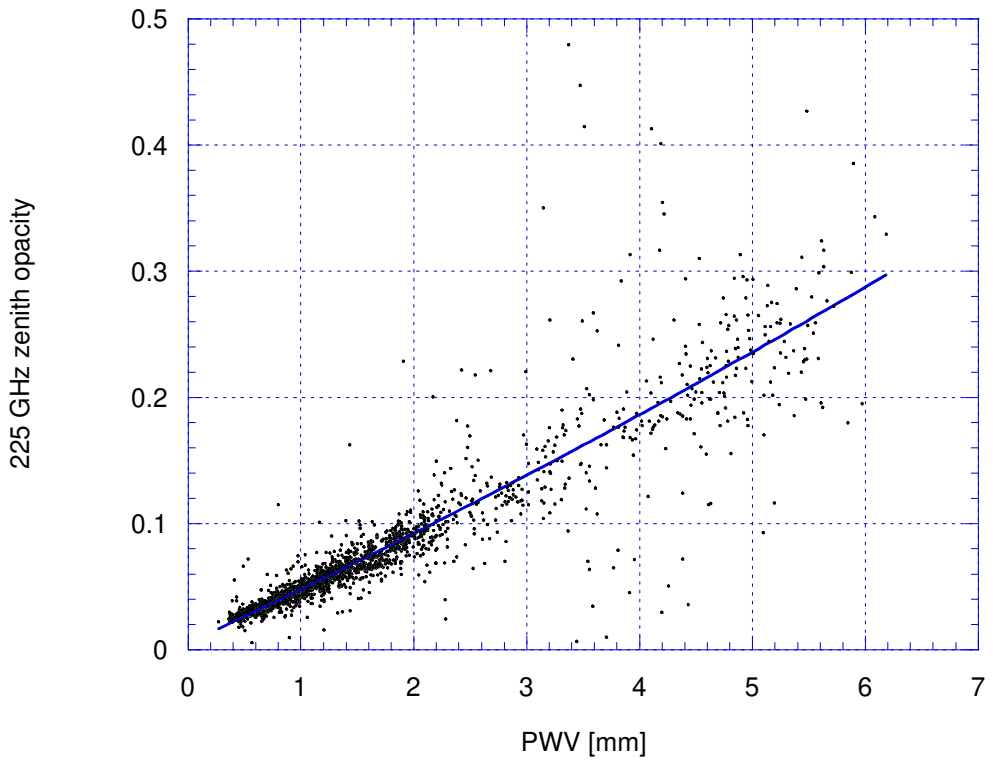

Fig.9 Correlation between the amount of *PWV* derived from 183 GHz radiometer measurements and zenith opacity measured at 225 GHz, the line is the second order polynomial fit to Liebe's 93 model [13] with a scale height of 2.0 km for the distribution of water vapour density.

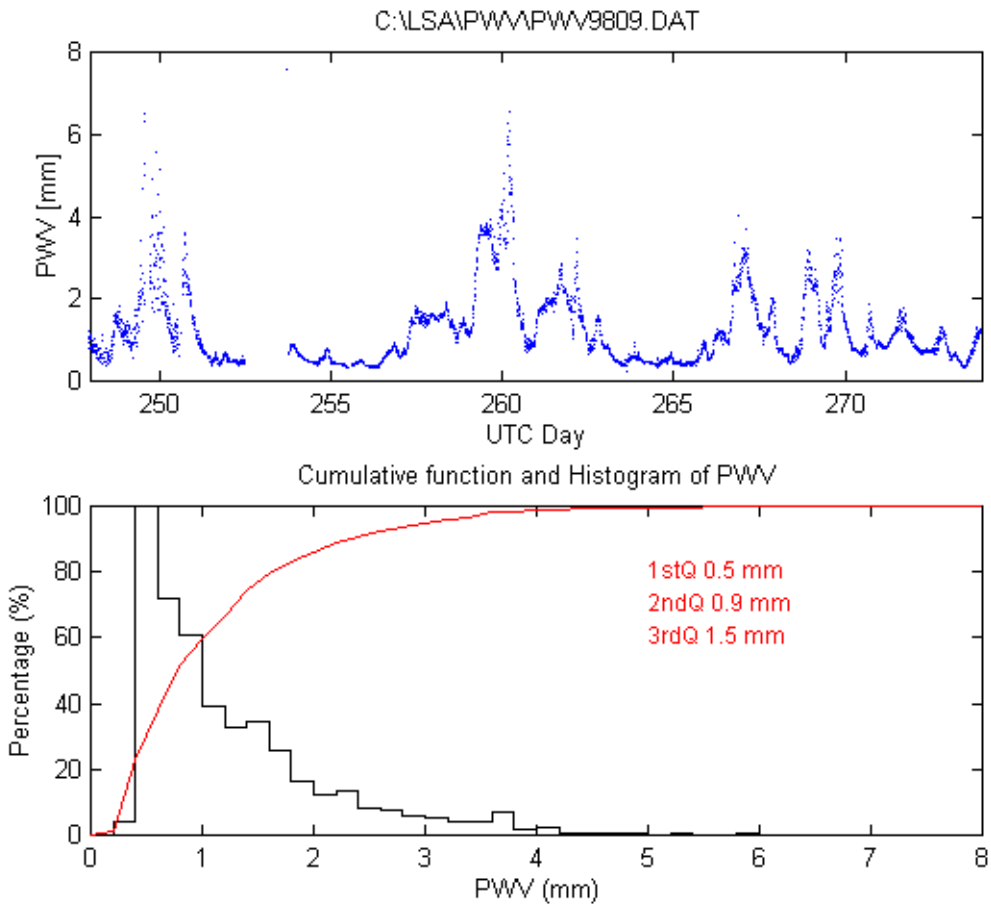

Fig.10 Amount of *PWV* determined from measurements at 183 GHz for the month of September (top diagram). Bellow is the cumulative distribution for the same period, with a median of 0.9 mm of *PWV*

Table 1: Weather sensors specifications

Sensor	Operating Range	Accuracy
Air Temperature	-30 – +70 ºC	0.2 ºC
Relative humidity	5 – 95%	1.5% in the range 5% to 60%
Solar radiation	0 – 1,100 W/m^2	±5% per Mjoule, spectral response 400 1,100 nm
Anemometer	0 – 150 km/h	0.5 m/s
Wind direction	0 – 360 degrees	3.0 degrees
Barometric pressure	740 – 490 mbar	±5 mbar